Lack of Aggregation of Molecules on Ice Nanoparticles

ARTICLE *in* THE JOURNAL OF PHYSICAL CHEMISTRY A · JULY 2015

Impact Factor: 2.69 · DOI: 10.1021/acs.jpca.5b05368 · Source: PubMed

8 AUTHORS, INCLUDING:

Alena Habartova

Academy of Sciences of the Czech Republic

8 PUBLICATIONS **12** CITATIONS

SEE PROFILE

Viktoriya Poterya

Academy of Sciences of the Czech Republic

52 PUBLICATIONS **727** CITATIONS

SEE PROFILE

Martina Roeselova

Academy of Sciences of the Czech Republic

46 PUBLICATIONS **891** CITATIONS

SEE PROFILE

Michal Fárník

Academy of Sciences of the Czech Republic

74 PUBLICATIONS **1,009** CITATIONS

SEE PROFILE

THE JOURNAL OF PHYSICAL CHEMISTRY A

Article

pubs.acs.org/JPCA

Lack of Aggregation of Molecules on Ice Nanoparticles

Andriy Pysanenko,[†] Alena Habartová,[*,‡] Pavla Svrčková,[†,§] Jozef Lengyel,[†,§] Viktoriya Poterya,[†] Martina Roeselová,[‡] Juraj Fedor,[*,†] and Michal Fárník[*,†]

[†]J. Heyrovský Institute of Physical Chemistry v.v.i., Czech Academy of Sciences, Dolejškova 3, 18223 Prague 8, Czech Republic

[‡]Institute of Organic Chemistry and Biochemistry v.v.i., Czech Academy of Sciences, Flemingovo nám. 2, 16610 Prague 6, Czech Republic

Supporting Information

ABSTRACT: Multiple molecules adsorbed on the surface of nanosized ice particles can either remain isolated or form aggregates, depending on their mobility. Such (non)-aggregation may subsequently drive the outcome of chemical reactions that play an important role in atmospheric chemistry or astrochemistry. We present a molecular beam experiment in which the controlled number of guest molecules is deposited on the water and argon nanoparticles in a pickup chamber and their aggregation is studied mass spectrometrically. The studied molecules (HCl, CH_3Cl, $CH_3CH_2CH_2Cl$, C_6H_5Cl, CH_4, and C_6H_6) form large aggregates on argon nanoparticles. On the other hand, no aggregation is observed on ice nanoparticles. Molecular simulations confirm the experimental results; they reveal a high degree of aggregation on the argon nanoparticles and show that the molecules remain mostly isolated on the water ice surface. This finding will influence the efficiency of ice grain-mediated synthesis (e.g., in outer space) and is also important for the cluster science community because it shows some limitations of pickup experiments on water clusters.

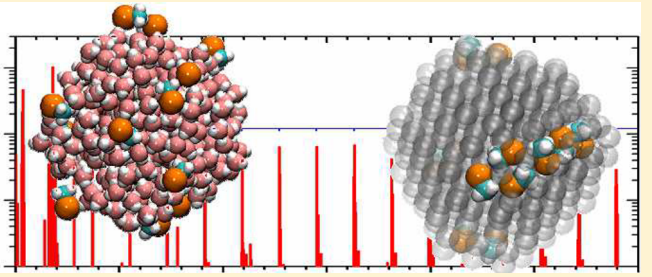

INTRODUCTION

Heterogeneous chemistry of molecules adsorbed on ice particles with nano- to micrometer dimensions plays a central role in several environments. An obvious example is photochemistry of halogenated species on polar stratospheric clouds and other ice particles in the atmosphere, where the presence of such nanoparticles triggers globally important chemical changes (ozone hole).[1] Also, it is believed that in outer space, where molecular density is very low, molecular ice particles (water ice in particular) represent "sponges" where guest molecules are adsorbed and meet other molecules yielding reactions, often assisted by high-energy radiation.[2,3]

One factor that will strongly influence both the photochemistry and ice-assisted synthesis is whether molecules remain isolated on the particle surface or form aggregates prior to the triggering radiation event. It can result in a dramatically different outcome of the subsequent reaction. The examples include the change in photochemistry of HCl in complexes when compared to that of monomers,[4] or cosmic-ray-induced glycine synthesis from simpler molecules on extraterrestrial ices.[3] The aggregation will be influenced by the molecules' mobility and migration upon their uptake on the particle. Surprisingly, few data about the molecular mobility on ice surfaces exists even for bulk ices.[5,6]

In laboratory experiments, the environments mentioned above are often mimicked by large water clusters (ice nanoparticles) with guest molecules adsorbed on their surface. The pickup technique that is used to adsorb the guest molecules on the clusters was introduced in 1980s by Gough et al.[7] A subsequent aggregation of adsorbed/embedded molecules has been exploited extensively for large superfluid helium nanodroplets[8−14] and to limited extent for argon nanoparticles.[4,15−19] We are not aware of any study addressing the question of aggregation on the surface of ice nanoparticles.

In this paper, we examine the aggregation of guest molecules on ice nanoparticles [water clusters $(H_2O)_N$, where $\bar{N} = 10^2-10^3$]. These particles have diameters in a nanometer range and possess low temperatures; as discussed in Computational Methods, we assume a temperature of ≈100 K. We successively dope the nanoparticles with a controlled number of guest molecules by pickup[20−22] and probe them mass spectrometrically. Surprisingly, no aggregation of guest molecules is observed. To examine the reliability of our technique and to provide a chemically inert reference, we perform analogous experiments with Ar_N clusters. In this case, strong aggregation of guest molecules is observed, in spite of the lower particle temperature of ≈37 K.[23] The experimental results are confirmed by molecular dynamics (MD) simulations. As the guest molecules, we study mainly Cl-containing species because of their atmospheric relevance. To probe different types of bonding, we proceed from diatomic HCl to chloroalkanes with various chain lengths (CH_3Cl and $CH_3CH_2CH_2Cl$) and to

Received: June 5, 2015
Revised: July 19, 2015

DOI: 10.1021/acs.jpca.5b05368
J. Phys. Chem. A XXXX, XXX, XXX−XXX

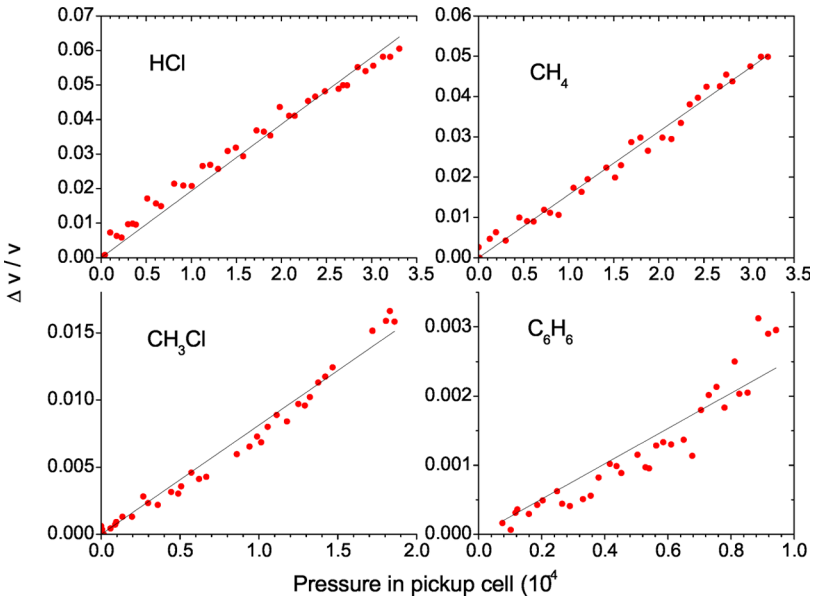

Figure 1. Dependence of the relative velocity decrease of the beam $\Delta v/v$ on pressure. Pickup on $(H_2O)_N$, $\bar{N} \approx 430$.

Table 1. Maximal Aggregate Fragment Sizes Observed in the Mass Spectra (m_{max}), Mean Numbers of Adsorbed Molecules (m_p) at Pressure p, and Maximal Aggregate Sizes from MD Simulations (m_{cal})[a]

		Ar_N			$(H_2O)_N$		
	p ($\times 10^{-4}$ mbar)	m_p	m_{max}	m_{cal}	m_p	m_{max}	m_{cal}
HCl	3.0	17(3)	11(2)	8(3)	17(5)	1	1
CH_4	3.3	22(2)	3(1)	2(1)	18(4)*	1	1
CH_3Cl	1.7	10(3)	7(2)	5(1)	4(2)	1	2(1)
C_3H_7Cl	0.9	7(1)	7(2)	4(1)	3(1)	1	3(1)
C_6H_6	0.9	4(2)**	9(1)	5(1)	1(1)**	1	2(1)
C_6H_5Cl	0.7	3(2)**	7(1)	5(1)	1(1)**	1	2(1)

[a]The numbers in parentheses correspond to standard deviations. The m_p value for methane on ice nanoparticles (one asterisk) is judged to be overestimated, and for benzene and chlorobenzene (two asterisks), both argon and ice have lower confidence levels (see the text).

aromatic compound C_6H_5Cl that can bind via π interactions. For comparison, nonpolar CH_4 and C_6H_6 molecules are also considered.

EXPERIMENTAL METHODS

The experiments were performed on the CLUster Beam apparatus (CLUB), which is a versatile molecular beam setup allowing for a range of experiments, including photochemistry, mass spectrometry, and pickup experiments with clusters and nanoparticles.[18,19,22,24] The Ar_N and $(H_2O)_N$ nanoparticles are generated in continuous supersonic expansion of Ar and water vapor, respectively, through a conical nozzle into the vacuum. The mean cluster size is controlled by the source conditions (stagnation pressure, temperature, and geometrical nozzle parameters). The present mean sizes are $\bar{N} \approx 330$ and 430 for Ar_N and $(H_2O)_N$, respectively. They correspond approximately to the same geometrical cross section of nanoparticles ($\sigma_g \approx 660$ Å^2), estimated assuming a spherical particle shape and density of the corresponding solid. The mean cluster size determination and calculation of geometrical cross section are described in the Supporting Information. The cluster beam is skimmed and passes through a differentially pumped chamber where the guest molecules are introduced.

In the first type of measurement, we determine the amount of picked up guest molecules from deceleration of the beam after it passes the pickup chamber. For this purpose, the beam velocity is determined by modulating the beam with a pseudorandom mechanical chopper and measuring its time of flight. The chopper is located in the next differentially pumped chamber after the pickup chamber, and the flight time is measured on a subsequent 151 cm path into a detector. There the clusters are ionized by 70 eV electrons, and ions selected by quadrupole analyzer are detected. The arrival time to the detector is measured and converted to the velocity distribution. Assuming that the cluster with the mass $\bar{N}M_C$ is slowed by picking up m_p guest molecules, the relative change of the cluster velocity is

$$\frac{\Delta v}{v} = \frac{M_M}{\bar{N}M_C} m_p \quad (1)$$

where M_M and M_C are masses of the guest molecule and cluster constituent, respectively. Despite the simplified assumptions (sticking collisions), this formula has been proven to deliver reliable results confirmed by molecular dynamics simulations of the pickup process for several species previously.[20−22] m_p is linearly dependent on the pickup cell pressure p, and consequently, $\Delta v/v = \alpha p$. Figure 1 shows typical pressure dependences of the relative deceleration $\Delta v/v$. The linear dependence was verified for each guest molecule, and m_p during subsequent mass spectrometry measurement (performed at a fixed p) was determined from measured slope α.

DOI: 10.1021/acs.jpca.5b05368
J. Phys. Chem. A XXXX, XXX, XXX−XXX

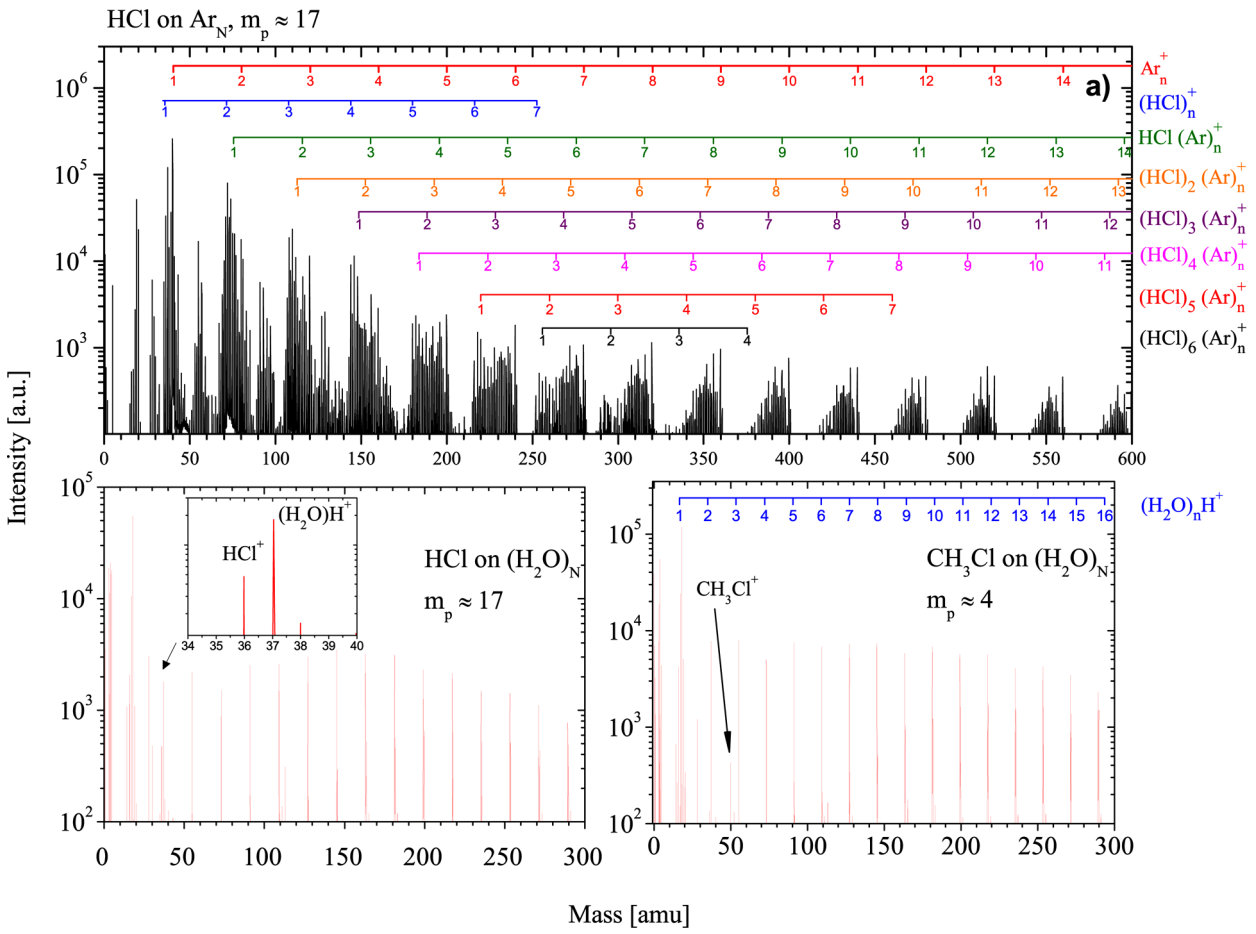

Figure 2. Representative time-of-flight mass spectra. The top panel shows HCl molecules adsorbed on argon nanoparticles with $\bar{N} \approx 330$. The bottom panels show HCl and CH_3Cl molecules adsorbed on water ice nanoparticles with $\bar{N} \approx 430$.

Pressure p was monitored with a Bayard-Alpert ionization gauge (Varian type 571). The measured pressures for various gases were divided by the correction factor listed in the gauge instruction manual. Because this is a crucial factor for m_p determination, we have calibrated the ionization gauge independently with a capacitance manometer (Pfeiffer CMR 365) and the absolute pressures were found to be in very good agreement with the corrected pressures based on the ionization gauge manual. The uncorrected pressure limit of the ionization gauge is 5×10^{-4} mbar, which for benzene and chlorobenzene leads to very low calibrated pressures (shown in Table 1) where the determination of α (and consequently of m_p) is subject to a relatively large error.

In the second type of measurement, the beam is not chopped, and we measure the mass spectra of the doped nanoparticles in another differentially pumped chamber with a high-resolution reflectron time-of-flight mass spectrometer (RTOF).[25−27] The RTOF is mounted orthogonally to the molecular beam. The clusters are ionized by 70 eV electrons at a 10 kHz repetition frequency, and the mass spectra are recorded with a resolution of $M/\Delta M \approx 5 \times 10^3$. In the perpendicular arrangement, attention must be paid to the mass discrimination because of the different cluster energies along the beam direction. The transmission of the spectrometer was checked with perfluorotributylamine (FC-43) and known spectra of large Ar_N clusters so that no discrimination occurs in the mass range up to $\sim 10^3$ amu.

COMPUTATIONAL METHODS

To provide further insight, we simulated motion of several guest molecules on both types of nanoparticles. Spherical nanoparticles consisting of 300 Ar atoms or H_2O molecules were carved out from a previously simulated liquid argon ($T \approx$ 100 K)/liquid water ($T \approx$ 300 K) system. Each nanoparticle was then placed in the center of a cubic simulation cell with an edge size of 80 Å (the diameters of the argon and water nanoparticles were ~30 Å). To equilibrate the nanoparticles to the known target temperature of 37 K (for argon)[23] and 100 K (for water),[28,29] 50 ns isochoric−isothermal (NVT) simulations were performed. The temperatures correspond to the experimental conditions. For argon nanoparticles created in supersonic expansion, the commonly accepted value is 37 K as measured by electron diffraction.[23] For water nanoparticles, a range of temperatures has been put forward: 180 ± 20 K was reported by electron diffraction experiment for $N < 200$,[30] temperatures between 50 and 100 K were estimated in a recent perspective,[29] and vibrational spectroscopy of size-selected nanoparticles with 200−500 molecules reported temperatures of 90−115 K.[31] We therefore assume a nanoparticle temperature of ≈100 K.

Subsequently, 12 identical molecules from the list of studied pickup species were added to the simulation cell. The molecules were initially evenly (pseudorandomly) distributed around the argon/amorphous ice nanoparticle several angstroms from the surface. The entire system was again shortly

DOI: 10.1021/acs.jpca.5b05368
J. Phys. Chem. A XXXX, XXX, XXX−XXX

equilibrated (≈10 ps) at the respective experimental temperature. During that period, most of the molecules landed on the surface, and the resulting configurations of the argon/amorphous ice nanoparticle with 12 adsorbed molecules were used as initial conditions for the subsequent production runs. The systems were propagated for 50 ns in the *NVT* simulation at the experimental temperatures given above to sample structural characteristics. Periodic boundary conditions were applied in all three dimensions. For each combination of the argon nanoparticle and the pickup species, five different initial configurations of molecules around the argon nanoparticle were created and the simulations were propagated independently. Close contacts of picked up molecules were considered as an aggregate (cluster) when no molecule of argon/H_2O was found between them.

Interaction Potentials. Water molecules were described using the TIP4*P*/2005 model,[32] while for argon, the OPLS parameters[33] were used. Topologies for the pickup molecules were obtained from the Automated Topology Builder,[34] and the general Amber force field (GAFF) parameter set[35] was employed to describe their interactions. Chemical bonds were kept intact during the simulations, including that in HCl (i.e., no acidic dissociation of molecular HCl on the clusters was considered, which will be discussed below). The atomic partial charges were calculated by the RESP method.[36] For CH_3Cl and C_6H_6, these charges were enhanced by factors of 1.7[37] and 1.24,[38] respectively. Further details of the theoretical simulations and the atomic partial charges and topologies of studied molecular species are attached as itp files in the Supporting Information.

RESULTS

Mass Spectra of Doped Nanoparticles. *Pickup on Ice Nanoparticles.* Bottom panels in Figure 2 show example mass spectra following the pickup of HCl and CH_3Cl on H_2O nanoparticles. Further spectra for all studied molecules are presented in the Supporting Information. The peak progression corresponds to protonated water cluster ions $(H_2O)_NH^+$. No ions corresponding to aggregates of guest molecules (either pure or mixed water−guest aggregates) were observed; only the monomer ions and their fragments are present in the spectra.

We are certain that these peaks originate from species deposited on the nanoparticles as the background signals measured with the blocked beam were carefully subtracted. The presence of molecules on ice nanoparticles was confirmed in some cases by our previous photodissociation studies[19,39,40] where features corresponding to nanoparticle−guest interactions (acidic dissociation) clearly dominate the spectra. Further evidence comes from the measured velocities shown in Figure 1. The increasing relative deceleration $\Delta v/v$ with pressure shows that the clusters are slowed by a momentum transfer from multiple guest molecules. Additionally, in a similar experiment, Ahmed and co-workers[41−43] reported sticking of a number of similar organic molecules on the surface of water clusters.

Pickup on Argon Nanoparticles. Mass spectra following pickup of guest molecules on argon nanoparticles are shown in the top panel of Figure 2 for HCl and in Figure 3 for CH_4, CH_3Cl, and $CH_3CH_2CH_2Cl$. Because of overlap of multiple spectra, a detailed analysis based on isotope ratios was required to assign all the mass peaks unambiguously. This analysis, as well as the mass spectra corresponding to the pickup of other guest molecules, is shown in the Supporting Information.

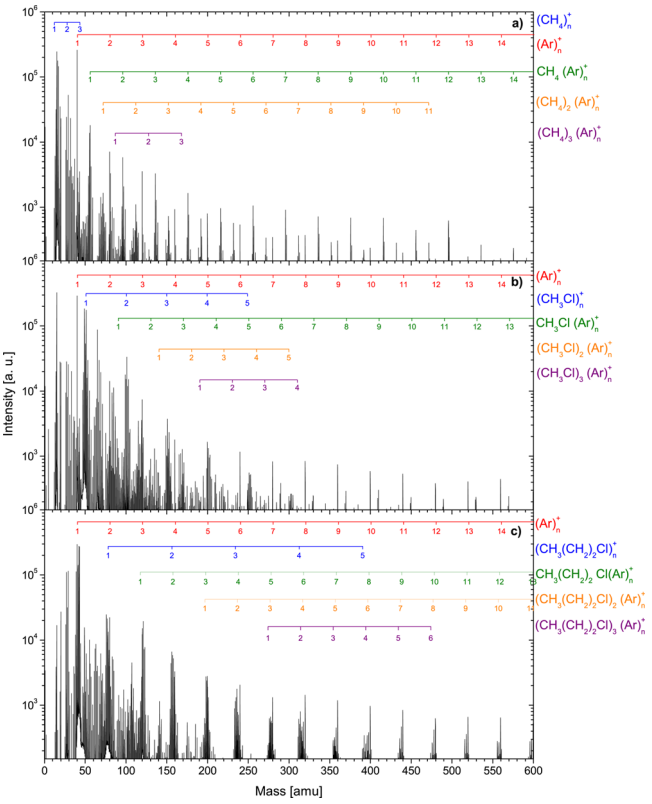

Figure 3. Mass spectrum of Ar_N, $\bar{N}$ = 330, clusters after the pickup of (a) CH_4 at $p = 2.0 \times 10^{-4}$ mbar, (b) CH_3Cl at $p = 1.0 \times 10^{-4}$ mbar, and (c) $CH_3CH_2CH_2Cl$ at $p = 0.6 \times 10^{-4}$ mbar. The series corresponding to the different cluster ion fragments are labeled.

As opposed to the ice nanoparticles, relatively large aggregate ions of the adsorbed molecules were observed on Ar_N: the mass spectra exhibited M_m^+ with $m \geq 10$ as well as mixed species $Ar_n \cdot M_k^+$. Figure 4 summarizes the mass peak intensities corresponding to M_m^+ cluster ions generated on Ar_N at the highest exploited pickup pressures. We denote the largest detected molecular cluster size as m_{max}. For the ice nanoparticles, m_{max} = 1 for all guest molecules. The results are summarized in Table 1.

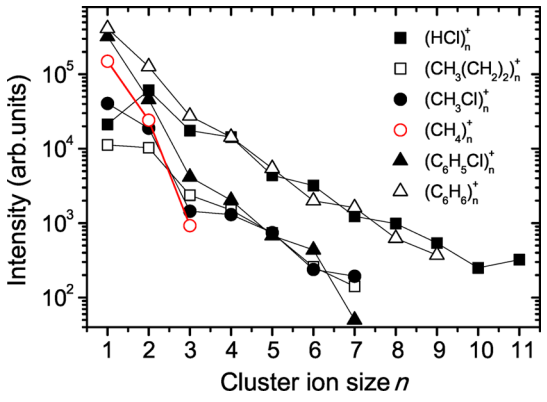

Figure 4. Mass peak intensities corresponding to M_n^+ aggregate ions following pickup of M on Ar_N nanoparticles ($\bar{N} \approx 330$).

For HCl, the mass spectra showed evidence of $(HCl)_m^+$ clusters up to the maximal cluster fragment size (m_{max}) of 11. For chloromethane also, relatively large $(CH_3Cl)_m^+$ cluster ions with m_{max} = 7 were observed. On the other hand, the clustering

DOI: 10.1021/acs.jpca.5b05368
J. Phys. Chem. A XXXX, XXX, XXX−XXX

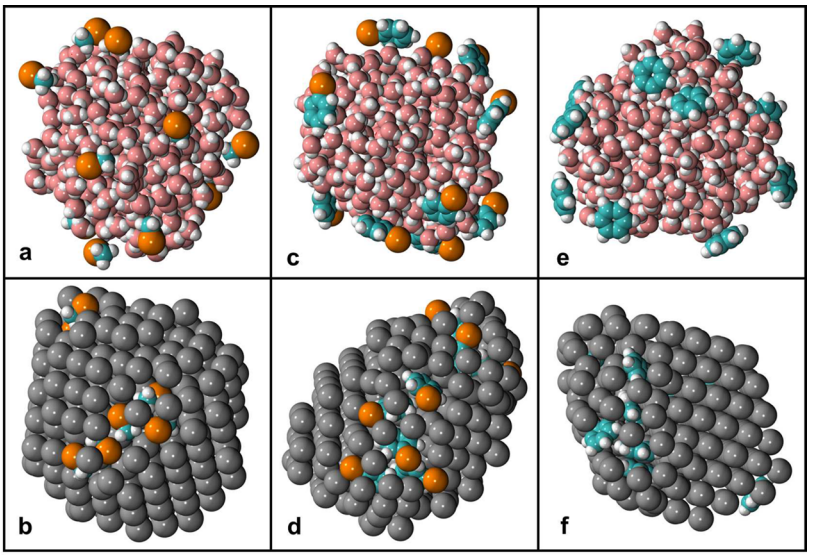

Figure 5. Last snapshots of the 50 ns MD simulation of ice (top) and argon (bottom) nanoparticles with 12 adsorbed pickup molecules: chloromethane (a and b), chlorobenzene (c and d), and benzene (e and f). Color coding: chlorine in orange, carbon in cyan, and hydrogen in white.

of a methane molecule on Ar_N was inefficient. Cluster fragments $(CH_4)_m^+$ were observed, but the maximal cluster size was only $m_{max} = 3$. This is nonetheless an interesting result. The fact that on the argon surface methane forms aggregates that do not decay completely upon the electron ionization opens experimental possibilities that are addressed in the Conclusions.

To investigate the influence of hydrocarbon chain length on molecule coagulation, we have studied the pickup of chloropropane where again the spectra exhibited large $(CH_3CH_2CH_2Cl)_m^+$ cluster ions up to $m_{max} = 7$. Because the linear chain length of the adsorbed molecule did not have any significant influence on the clustering on Ar_N, we exploited aromatic molecules chlorobenzene (C_6H_5Cl) and benzene (C_6H_6), if the interaction of the ring π electrons would change the coagulation behavior. However, the spectra exhibit essentially the same clustering as the linear molecules described above: large $(C_6H_6)_m^+$ fragments with $m_{max} = 9$ for benzene and $(C_6H_5Cl)_m^+$ with $m_{max} = 7$ for chlorobenzene.

MD Simulations. The MD simulations were performed for 50 ns to visualize possible coagulation of 12 individual molecules of the tested molecules on Ar_N or $(H_2O)_N$ (N = 300) nanoparticles. Within the first 10 ps, the guest molecules were adsorbed on the nanoparticle surfaces. Once adsorbed, they remained so on argon or ice for the entire simulation run. The only exceptions were the molecules of HCl and methane, which underwent desorption/absorption cycles on amorphous ice. In a 50 ns period, an isolated molecule of HCl desorbed approximately four times while an isolated CH_4 molecule desorbed ~200 times. However, for HCl, one has to consider that the molecule acidically dissociates on the ice nanoparticles, which has not been taken into account in simulations presented here (see Discussion). All the other adsorbed molecules were moving on the nanoparticle surface roughly for the first 10 ns. During this period, molecular aggregates were formed and submerged, and a practically final orientation of the molecules took place. For the next 40 ns, the molecules remained mostly fixed, except for benzene aggregates being submerged in the argon nanoparticle. Figure 5 shows several snapshots at the end of the simulation (see the Supporting Information for further snapshots and videos).

Coagulation on Argon. All studied molecules formed aggregates on argon (Figure 5). To eliminate the influence of the initial conditions, for each molecular species several separate simulations were run and the maximal cluster size was determinated from the last snapshot. HCl molecules created molecular chains with an average maximal size of eight molecules. Methyl chloride and propyl chloride generated on average clusters of five and four molecules, respectively. Benzene (without a dipole moment) and chlorobenzene (dipole moment of 2.1 D) coagulate to the same extent (average maximal size m_{cal} = 5 molecules). This points to the dominant role of π interaction of aromatic rings. The largest aggregates of methane consisted on average of only two molecules (Table 1). Interestingly, chloromethanes, chlorobenzenes, and benzenes were submerged in argon nanoparticles, while chloropropanes remained localized more at the surface. Chlorine atoms of both chloropropane and chlorobenzene were mostly oriented outside of the argon cluster.

Coagulation on Ice. We observe mostly individual molecules on the $(H_2O)_N$ ice nanoparticles because the picked up molecules do not aggregate. Only chloromethane, benzene, and chlorobenzene formed in each simulation one dimer, and chloropropane formed one trimer. The nonaggregation on the ice particles results from a combination of kinetic and thermodynamic effects. The interaction of guest molecules with polar water molecules inhibits their mobility. They generally remain at the position of the first contact with the surface and merely reorient themselves with respect to the closest water molecules (kinetic effect). A similar finding has been observed experimentally for chloroform $(CHCl_3)$ molecules that remain immobile on the bulk ice surface up to the desorption temperature.[5] Additionally, the amorphous surface layer effectively solvates the guest molecule, and in some cases, this solvation prevents aggregation of guest molecules in spite of their physical proximity (thermodynamic effect).

DOI: 10.1021/acs.jpca.5b05368
J. Phys. Chem. A XXXX, XXX, XXX−XXX

DISCUSSION

The unambiguous experimental observation is that while large aggregate ions of guest molecules M are detected from argon nanoparticles, both pure M_n^+ and mixed $M_n \cdot Ar_m^+$ ions, only the monomer ions are detected from the ice nanoparticles. To be certain that this observation leads to the conclusion outlined in the title of this paper, several issues have to be addressed. First, we have to consider the possibility of electron-induced aggregate fragmentation. Generally, the electron impact ionization in the gas phase leads to strong fragmentation, which allows speculation that molecular aggregates on ice particles could be formed but are decomposed in the ionization process. Even though we cannot fully exclude a certain amount of fragmentation, there is a strong evidence that ionization is much softer when the aggregate is on the surface of a nanoparticle. This is clearly experimentally demonstrated in this work in the case of argon nanoparticles upon comparison of m_p and m_{max} in Table 1. The number of picked up molecules (m_p) corresponds to the cluster ion size observed on Ar_N. This shows that molecules coagulate efficiently into their aggregates and a certain fraction of these aggregates does not fragment upon ionization. The reason is that the nanoparticle serves as an efficient heat bath and can dissipate the excess energy upon ionization, e.g., via evaporation of Ar atoms. Second, the ionization on nanoparticles is less destructive, because it can proceed via ionization of an argon atom and a subsequent charge transfer process to the guest molecule with release of much less excess energy than a direct ionization.[26,27] It should be noted that the mass peak intensities in Figure 4 do not follow a Poisson distribution, which describes the number of picked up molecules.[20] This points to a certain degree of fragmentation. However, the mass peak intensities are determined not only by the eventual fragmentation but also by the aggregate size distribution before the ionization event, i.e., degree of coagulation, which is difficult to predict.

We are aware of only one experimental confirmation of soft ionization for molecules deposited on ice nanoparticles: Moro et al.[44,45] reported almost negligible fragmentation of amino acids after they were picked up on water clusters, in contrast to rich fragmentation patterns of these molecules in the gas phase. The excess energy transfer to the water solvent can be even more efficient than in the argon case because the water molecules pose internal degrees of freedom, where the energy can be transferred. Besides, a lower ionization energy of water compared to that of argon leads to less excess energy in case of the host molecule/cluster ionization by charge transfer from water or argon. In addition, relatively soft proton transfer ionization is possible in $(H_2O)_N$. It is thus reasonable to assume soft ionization of aggregates on the surface of ice nanoparticles.

Another critical factor is the number of picked up molecules (m_p). Its determination relies on two assumptions about the deceleration of nanoparticles in the pickup chamber: (i) the sticking collisions during which guest molecules land on the surface are the dominant contributor to the momentum transfer, and (ii) guest molecules do not spontaneously desorb. We have previously shown[20−22] by extensive Monte Carlo simulations that assumption (i) is fulfilled for both argon and water particles; the statistical weight of nonsticking scattering events is much smaller than that of the sticking events. The relatively low collision energies (undisturbed beam velocities being 1450 ms^{-1} for H_2O and 490 ms^{-1} for Ar particles) lead to "soft landing" on the particle surface. Assumption (ii) is verified in the MD simulations presented here. The guest molecules, once adsorbed, remained on the surface of both argon or ice for the entire simulation run, with two exceptions, HCl and CH_4, as described above. Therefore, the m_p value for methane can be overestimated. This is also suggested by the negligible intensity of the methane peaks in the mass spectra (Supporting Information). The situation is different for HCl, which has been shown experimentally to undergo acidic dissociation to the $Cl^- \cdot H_3O^+$ ion pair on ice nanoparticles.[19,39,40,46] A simulation of this process goes beyond the MD model presented here, in which the chemical bonds were kept intact. Acidic dissociation will prohibit desorption of HCl from the surface and probably further inhibit the aggregation of the guest molecules. Thus, the determination of the m_p for HCl is reliable. As for the possible desorption of other guest molecules, it should be noted that MD simulations probe a time scale that is approximately 5 orders of magnitude shorter than the experimental time window and thus do not fully exclude the possibility of desorption in the experiment. However, in our previous systematic investigation of chloroalkanes at liquid water interfaces, we have shown that the free energy profiles have minima at the water−vapor interface and molecules prefer to stay adsorbed on the water surface even at 300 K.[37] The present, much lower temperature will only decrease the desorption probability.

For benzene and chlorobenzene on argon nanoparticles, the m_p values are lower than m_{max}. This is possible because m_p is a mean number of picked up molecules; their actual number follows a Poisson distribution[20] and can be larger. However, we consider these m_p values to be underestimated; no other molecule shows $m_{max} > m_p$, and the pickup chamber pressures for these two molecules are low because of high correction factors. All pressures in Table 1 correspond to the maximal reliable pressure of the ionization gauge of 5×10^{-4} mbar. The slope determination of the $\Delta v/v$ pressure dependence (described in the Supporting Information) at these low pressures has large error bars.

These MD simulations were actually inspired by the experimental results and were performed to account for the main uncertainty in the experimental interpretation, regardless of whether the lack of observation of aggregate ions in the mass spectra on ice nanoparticle can be interpreted as the lack of neutral aggregates prior to the ionization. As described in Results, they fully support this interpretation. Again, the shorter time scale of the simulations when compared with that of the experiment comes into question. The degree of aggregation would be strongly influenced by a time scale if it were limited solely by the mobility of guest molecules on the particle. However, the low mobility on the ice surface is only part of the reason for the nonaggregation. We have observed a number of trajectories in which two guest molecules came into physical proximity of each other on the ice surface but did not form dimers because they were solvated by water molecules. The important role of binding of guest molecules to water has been pointed out by Ahmed and co-workers.[42,43] The fact that the guest molecules remain on the surface and are not submerged in the nanoparticle can be attributed to the fact that guest−H_2O interaction is weaker than H_2O−H_2O interaction. On the other hand, the guest−H_2O and guest−guest interaction energies have similar magnitudes, which leads to surface solvation of the guest molecules. The detailed analysis of energetics and the temperature dependence of the mobility and

DOI: 10.1021/acs.jpca.5b05368
J. Phys. Chem. A XXXX, XXX, XXX−XXX

aggregation process will be a subject of a separate theoretical publication.

CONCLUSIONS

In conclusion, we have shown experimentally that adsorption of multiple molecues on the surface of water ice nanoparticles and the subsequent ionization do not lead to formation of any aggregate ions. MD simulations confirm that the molecules stay mostly isolated and do not form aggregates in spite of their physical proximity. This is in strong contrast with their behavior on the surface of argon nanoparticles, where they are mobile and coagulate efficiently. In the mass spectra, this is reflected in a rich progression of either pure aggregate or mixed aggregate−argon ions. Even methane after adsorption on argon and ionization forms pure aggregates $(CH_4)_n^+$ up to $n = 3$. Methane is known to be a difficult gas to cluster in co-expansions probably due to its small c_p/c_v ratio.[47] The use of argon nanoparticles as a cold support could represent a way to generate interesting methane-containing aggregates, e.g., clathrates. An additional interesting result for doped argon nanoparticles is shown by MD simulations: while some of the aggregates are submerged into the nanoparticle (chloromethanes, chlorobenzenes, and benzenes), some remain on its surface (methane and chloropropane). Choropropane and chlorobenzene are oriented with chlorine atoms pointing out of the surface. These two findings will have consequences for the amount of caging observed in future photodissociation studies.

With respect to the implications in astro- and atmospheric chemistry outlined in the Introduction, it is important to note that these findings apply to water ices with temperature around 100 K and an amorphous surface layer.[48] Naturally occurring nano- to microsized ices encompass a range of temperatures in different regions. The time scales should also not be overlooked: experimentally, we probed processes on a millisecond time scale, theoretically on a nanosecond time scale, while for example, the interstellar chemistry often requires millions of years. These results are also of fundamental interest to the cluster physics research. Rare gas nanoparticles or helium nanodroplets are often used as a support for forming cold clusters of picked-up molecules. This will be apparently difficult with water clusters. Several research groups have envisioned the use of water clusters as a supporting microsolvation system, e.g., for providing support for Watson−Crick pair formation by successive pickup of nucleobases. The low mobility and nonaggregation of guest molecules can represent an obstructive factor for such approach. A more promising way to generate such species would be co-expansion with the water vapor instead of the pickup, which has been demonstrated for a number of biomolecules.[49−51] However, in such a case, the molecules are generally incorporated into the bulk water and composition of the resulting nanoparticles (number of water molecules vs number of "guest" molecules) is difficult to control.

ASSOCIATED CONTENT

Supporting Information

The Supporting Information is available free of charge on the ACS Publications website at DOI: 10.1021/acs.jpca.5b05368.

Detailed description of the experiment, expansion conditions, and geometrical cross sections (PDF)

Detailed analysis of mass spectra and their discussion (ZIP)

Topology file and video with the final configurations from a MD simulation (MPG)

Topology file and video with the final configurations from a MD simulation (MPG)

Topology file and video with the final configurations from a MD simulation (MPG)

Topology file and video with the final configurations from a MD simulation (MPG)

Topology file and video with the final configurations from a MD simulation (MPG)

Topology file and video with the final configurations from a MD simulation (MPG)

Topology file and video with the final configurations from a MD simulation (MPG)

Topology file and video with the final configurations from a MD simulation (MPG)

Topology file and video with the final configurations from a MD simulation (MPG)

Topology file and video with the final configurations from a MD simulation (MPG)

Topology file and video with the final configurations from a MD simulation (MPG)

Topology file and video with the final configurations from a MD simulation (MPG)

AUTHOR INFORMATION

Corresponding Authors

*E-mail: alena.habartova@marge.uochb.cas.cz.

*E-mail: juraj.fedor@jh-inst.cas.cz.

*E-mail: michal.farnik@jh-inst.cas.cz.

Present Address

§P.S. and J.L.: Department of Physical Chemistry, University of Chemistry and Technology, Technická 5, 16628 Prague 6, Czech Republic.

Notes

The authors declare no competing financial interest.

ACKNOWLEDGMENTS

This work has been supported by Czech Science Foundation Projects 15-12386S and 13-06181S. We thank Prof. Pavel Jungwirth, Prague, for fruitful discussions.

REFERENCES

(1) Peter, T. Microphysics and Heterogeneous Chemistry of Polar Stratospheric Clouds. *Annu. Rev. Phys. Chem.* **1997**, *48*, 785−822.

(2) Herbst, E.; van Dishoeck, E. F. Complex Organic Interstellar Molecules. *Annu. Rev. Astron. Astrophys.* **2009**, *47*, 427−480.

(3) Holtom, P. D.; Bennett, C. E.; Osamura, Y.; Mason, N. J.; Kaiser, R. I. A Combined Experimental and Theoretical Study on the Formation of the Amino Acid Glycine and its Isomer in Extraterrestrial Ices. *Astrophys. J.* **2005**, *626*, 940−952.

(4) Nahler, N. H.; Fárník, M.; Buck, U.; Vach, H.; Gerber, R. B. Photodissociation of HCl and Small $(HCl)_m$ Complexes in and on Large Ar_n Clusters. *J. Chem. Phys.* **2004**, *121*, 1293−1302.

(5) Grecea, M.; Backus, E.; Fraser, H.; Pradeep, T.; Kleyn, A.; Bonn, M. Mobility of Haloforms on Ice Surfaces. *Chem. Phys. Lett.* **2004**, *385*, 244−248.

(6) Park, S. C.; Moon, K. S.; Kang, H. Some Fundamental Properties and Reactions of Ice Surfaces at Low Temperatures. *Phys. Chem. Chem. Phys.* **2010**, *12*, 12000−12011.

(7) Gough, T. E.; Mengel, M.; Rowntree, P. A.; Scoles, G. Infrared Spectroscopy at the Surface of Clusters: SF_6 on Ar. *J. Chem. Phys.* **1985**, *83*, 4958−4961.

DOI: 10.1021/acs.jpca.5b05368
J. Phys. Chem. A XXXX, XXX, XXX−XXX

(8) Lewerenz, M.; Schilling, B.; Toennies, J. P. Successive Capture and Coaugulation of Atoms and Molecules to Small Clusters in Large Liquid Helium Clusters. *J. Chem. Phys.* **1995**, *102*, 8191−8207.
(9) Behrens, M.; Fröchtenicht, R.; Hartmann, M.; Siebers, J. G.; Buck, U.; Hagemeister, F. C. Vibrational Spectroscopy of Methanol and Acetonitrile clusters in Cold Helium Droplets. *J. Chem. Phys.* **1999**, *111*, 2436−2443.
(10) Scoles, G.; Lahmann, K. K. Nanomatrices are Cool. *Science* **2000**, *287*, 2429−2430.
(11) Toennies, J. P.; Vilesov, A. F. Superfluid Helium Droplets: A Uniquely Cold Nanomatrix for Molecules and Molecular Complexes. *Angew. Chem., Int. Ed.* **2004**, *43*, 2622−2648.
(12) Choi, M.; Miller, R. Infrared Laser Spectroscopy of Imidazole Complexes in Helium Nanodroplets: Monomer,Dimer, and Binary Water Complexes. *J. Phys. Chem. A* **2006**, *110*, 9344−9351.
(13) Denifl, S.; Zappa, F.; Mähr, I.; da Silva, F. F.; Aleem, A.; Mauracher, A.; Probst, M.; Urban, J.; Mach, P.; Bacher, A.; et al. Ion−Molecule Reactions in Helium Nanodroplets Doped with C_60 and Water Clusters. *Angew. Chem.* **2009**, *121*, 9102−9105.
(14) Lehnig, R.; Sebree, J. A.; Slenczka, A. Structure and Dynamics of Phthalocyanine-Argon$_n$ (n = 1−4) Complexes Studied in Helium Nanodroplets. *J. Phys. Chem. A* **2007**, *111*, 7576−7584.
(15) Huisken, F.; Stemmler, M. Infrared Spectroscopy of Methanol Clusters Adsorbed on Large Ar$_x$ Host Clusters. *J. Chem. Phys.* **1993**, *98*, 7680.
(16) Ehbrecht, M.; Stemmler, M.; Huisken, F. Enhanced Production of Unprotonated Hydrogen-bonded Cluster Ions. *Int. J. Mass Spectrom. Ion Processes* **1993**, *123*, R1.
(17) Fedor, J.; Kočišek, J.; Poterya, V.; Votava, O.; Pysanenko, A.; Lipciuc, L.; Kitsopoulos, T. N.; Fárník, M. Velocity Map Imaging of HBr Photodissociation in Large Rare Gas Clusters. *J. Chem. Phys.* **2011**, *134*, 154303.
(18) Poterya, V.; Kočišek, J.; Lengyel, J.; Svrčková, P.; Pysanenko, A.; Hollas, D.; Slavíček, P.; Fárník, M. Clustering and Photochemistry of Freon CF2Cl2 on Argon and Ice Nanoparticles. *J. Phys. Chem. A* **2014**, *118*, 4740−4749.
(19) Poterya, V.; Lengyel, J.; Pysanenko, A.; Svrčková, P.; Fárník, M. Imaging of Hydrogen Halides Photochemistry on Argon and Ice Nanoparticles. *J. Chem. Phys.* **2014**, *141*, 074309.
(20) Fedor, J.; Poterya, V.; Pysanenko, A.; Fárník, M. Cluster Cross Sections from Pickup Measurements: Are the Established Methods Consistent? *J. Chem. Phys.* **2011**, *135*, 104305.
(21) Lengyel, J.; Kočišek, J.; Poterya, V.; Pysanenko, A.; Svrčková, P.; Fárník, M.; Zaouris, D.; Fedor, J. Uptake of Atmospheric Molecules by Ice Nanoparticles: Pickup Cross Sections. *J. Chem. Phys.* **2012**, *137*, 034304.
(22) Lengyel, J.; Pysanenko, A.; Poterya, V.; Slavíček, P.; Fárník, M.; Kočišek, J.; Fedor, J. Irregular Shapes of Water Clusters Generated in Supersonic Expansions. *Phys. Rev. Lett.* **2014**, *112*, 113401.
(23) Farges, J.; de Feraudy, M. F.; Raoult, B.; Torchet, G. Structure and Temperature of Rare Gas Clusters in a Supersonic Expansion. *Surf. Sci.* **1981**, *106*, 95.
(24) Poterya, V.; Kočišek, J.; Pysanenko, A.; Fárník, M. Caging of Cl Atoms from Photodissociation of CF_2Cl_2 in Clusters. *Phys. Chem. Chem. Phys.* **2014**, *16*, 421−429.
(25) Lengyel, J.; Pysanenko, A.; Kočišek, J.; Poterya, V.; Pradzynski, C.; Zeuch, T.; Slavíček, P.; Fárník, M. Nucleation of Mixed Nitric Acid-Water Ice Nanoparticles in Molecular Beams that Starts with a HNO_3 Molecule. *J. Phys. Chem. Lett.* **2012**, *3*, 3096−3109.
(26) Kočišek, J.; Lengyel, J.; Fárník, M. Ionization of Large Homogeneous and Heterogeneous Clusters Generated in Acetylene Ar Expansions: Cluster Ion Polymerization. *J. Chem. Phys.* **2013**, *138*, 124306.
(27) Kočišek, J.; Lengyel, J.; Fárník, M.; Slavíček, P. Energy and Charge Transfer in Ionized Argon Coated Water Clusters. *J. Chem. Phys.* **2013**, *139*, 214308.
(28) Jansen, R.; Wysong, I.; Gimelshein, S.; Zeifman, M.; Buck, U. Nonequilibrium Numerical Model of Homogeneous Condensation in Argon and Water Vapor Expansions. *J. Chem. Phys.* **2010**, *132*, 244105.
(29) Buck, U.; Pradzynski, C. C.; Zeuch, T.; Dieterich, J. M.; Hartke, B. A Size Resolved Investigation of Large Water Clusters. *Phys. Chem. Chem. Phys.* **2014**, *16*, 6859−6871.
(30) Torchet, G.; Schwartz, P.; Farges, J.; de Feraudy, M. F.; Raoult, B. Structure of Solid Water Clusters Formed in a Free Jet Expansion. *J. Chem. Phys.* **1983**, *79*, 6196−6202.
(31) Pradzynski, C. C.; Forck, R. M.; Zeuch, T.; Slavíček, P.; Buck, U. A Fully Size-Resolved Perspective on the Crystallization of Water Clusters. *Science* **2012**, *337*, 1529−1532.
(32) Abascal, J. L. F.; Vega, C. A General Purpose Model for the Condensed Phases of Water: TIP4P/2005. *J. Chem. Phys.* **2005**, *123*, 234505.
(33) Kaminski, G. A.; Friesner, R. A.; Tirado-Rives, J.; Jorgensen, W. L. Evaluation and Reparametrization of the OPLS-AA Force Field for Proteins via Comparison with Accurate Quantum Chemical Calculations on Peptides. *J. Phys. Chem. B* **2001**, *105*, 6474−6487.
(34) Malde, A. K.; Zuo, L.; Breeze, M.; Stroet, M.; Poger, D.; Nair, P. C.; Oostenbrink, C.; Mark, A. E. An Automated Force Field Topology Builder (ATB) and Repository: Version 1.0. *J. Chem. Theory Comput.* **2011**, *7*, 4026−4037.
(35) Wang, J.; Wolf, R. M.; Caldwell, J. W.; Kollman, P. A.; Case, D. A. Development and Testing of a General Amber Force Field. *J. Comput. Chem.* **2004**, *25*, 1157−1174.
(36) Bayly, C. I.; Cieplak, P.; Cornell, W.; Kollman, P. A. A Well-Behaved Electrostatic Potential Based Method Using Charge Restraints for Deriving Atomic Charges: the RESP Model. *J. Phys. Chem.* **1993**, *97*, 10269−10280.
(37) Habartová, A.; Valsaraj, K. T.; Roeselová, M. Molecular Dynamics Simulations of Small Halogenated Organics at the Air-Water Interface: Implications in Water Treatment and Atmospheric Chemistry. *J. Phys. Chem. A* **2013**, *117*, 9205−9215.
(38) Vácha, R.; Jungwirth, P.; Chen, J.; Valsaraj, K. Adsorption of Polycyclic Aromatic Hydrocarbons at the Air-Water Interface: Molecular Dynamics Simulations and Experimental Atmospheric Observations. *Phys. Chem. Chem. Phys.* **2006**, *8*, 4461−4467.
(39) Poterya, V.; Fárník, M.; Slavíček, P.; Buck, U.; Kresin, V. V. Photodissociation of Hydrogen Halide Molecules on Free Ice Nanoparticles. *J. Chem. Phys.* **2007**, *126*, 071101.
(40) Poterya, V.; Fedor, J.; Pysanenko, A.; Tkáč, O.; Lengyel, J.; Ončák, M.; Slavíček, P.; Fárník, M. Photochemistry of HI on Argon and Water Nanoparticles: Hydronium Radical Generation in HI·$(H_2O)_n$. *Phys. Chem. Chem. Phys.* **2011**, *13*, 2250−2258.
(41) Ahmed, M.; Apps, C. J.; Hughes, C.; Whitehead, J. C. The Adsorption of Methanol on Large Water Clusters. *Chem. Phys. Lett.* **1995**, *240*, 216−219.
(42) Ahmed, M.; Apps, C. J.; Hughes, C.; Watt, N. E.; Whitehead, J. C. Adsorption of Organic Molecules on Large Water Clusters. *J. Phys. Chem. A* **1997**, *101*, 1250−1253.
(43) Ahmed, M.; Apps, C. J.; Buesnel, R.; Hughes, C.; Hillier, I. H.; Watt, N. E.; Whitehead, J. C. Adsorption of NxOy-Based Molecules on Large Water Clusters: An Experimental and Theoretical Study. *J. Phys. Chem. A* **1997**, *101*, 1254−1259.
(44) Moro, R.; Rabinovitch, R.; Kresin, V. V. Amino-acid and Water Molecules Adsorbed on Water Clusters in a Beam. *J. Chem. Phys.* **2005**, *123*, 074301.
(45) Moro, R.; Rabinovitch, R.; Kresin, V. V. Pickup Cell for Cluster Beam Experiments. *Rev. Sci. Instrum.* **2005**, *76*, 156104.
(46) Ončák, M.; Slavíček, P.; Fárník, M.; Buck, U. Photochemistry of Hydrogen Halides on Water Clusters: Simulations of Electronic Spectra and Photodynamics, and Comparison with Photodissociation Experiments. *J. Phys. Chem. A* **2011**, *115*, 6155−6168.
(47) Ding, A.; Cassidy, R. A.; Futrell, J. H.; Cordis, L. Ion−molecule Reactions within Methane Clusters Initiated by Photoionization. *J. Phys. Chem.* **1987**, *91*, 2562−2568.
(48) Buch, V.; Bauerecker, S.; Devlin, J. P.; Buck, U.; Kazimirski, J. K. Solid Water Clusters in the Size Range of Tens-Thousands of H2O: a Combined Computational/Spectroscopic Outlook. *Int. Rev. Phys. Chem.* **2004**, *23*, 375−433.

DOI: 10.1021/acs.jpca.5b05368
J. Phys. Chem. A XXXX, XXX, XXX−XXX

709 (49) Kim, S. K.; Lee, W.; Herschbach, D. R. Cluster Beam
710 Chemistry: Hydration of Nucleic Acid Bases; Ionization Potentials
711 of Hydrated Adenine and Thymine. *J. Phys. Chem.* **1996**, *100*, 7933−
712 7937.
713 (50) Belau, L.; Wilson, K. R.; Leone, S. R.; Ahmed, M. Vacuum-
714 Ultraviolet Photoionization Studies of the Microhydration of DNA
715 Bases (Guanine, Cytosine, Adenine, and Thymine). *J. Phys. Chem. A*
716 **2007**, *111*, 7562−7568.
717 (51) Nosenko, Y.; Kunitski, M.; Riehn, C.; Harbach, P. H. P.; Dreuw,
718 A.; Brutschy, B. The Structure of Adenine Monohydrates Studied by
719 Femtosecond Multiphoton Ionization Detected IR Spectroscopy and
720 Quantum Chemical Calculations. *Phys. Chem. Chem. Phys.* **2010**, *12*,
721 863−870.

DOI: 10.1021/acs.jpca.5b05368
J. Phys. Chem. A XXXX, XXX, XXX−XXX